Ion radiation induced diffusion of Xe implanted into a polymer film

J. R. Kaschny, L. Amaral, M. Behar, and D. Fink

Citation: Journal of Applied Physics **72**, 5139 (1992); doi: 10.1063/1.352044
View online: http://dx.doi.org/10.1063/1.352044
View Table of Contents: http://scitation.aip.org/content/aip/journal/jap/72/11?ver=pdfcov
Published by the AIP Publishing

Ion radiation induced diffusion of Xe implanted into a polymer film

J. R. Kaschny and L. Amaral
Instituto de Física, Universidade Federal do Rio Grande do Sul, 91500 Porto Alegre, RS, Brasil

M. Behar
Instituto de Física, Universidade Federal do Rio Grande do Sul, 91500 Porto Alegre, RS, Brasil

D. Fink
Hahn–Meitner Institut für Kernforschung, D 1000 Berlin, Germany

(Received 26 May 1992; accepted for publication 17 August 1992)

In the present work, we have studied the most important parameters which can influence the radiation induced diffusion mechanism of Xe ions implanted into a photoresist film. With this aim, we have Ar post-bombarded the Xe implanted samples at a fixed Ar ion energy, covering a wide range of fluences. In addition, the implantation fluences, as well as the ion species used in the bombardment, were changed. The results show that the radiation induced diffusion process undergoes a trapping-detrapping mechanism. The trapping probability is proportional to the implanted fluence, and the detrapping one depends on the kind of ion used in the bombarding experiment. Finally, it is shown that the nuclear energy transfer plays an important role in the radiation induced diffusion mechanism.

I. INTRODUCTION

In the last years we have performed a systematic depth profile study for a variety of ions ($5 < Z < 83$) implanted in polymers.[1,2] Most of the elements exhibit regular profiles with range parameters well reproduced by the calculation of Ziegler, Biersack, and Littmark[3] via the Monte Carlo TRIM code.[4] The exceptions are light ions[5,6] and noble gases.[7]

In particular, it was found that He diffuses rapidly when implanted into Mylar,[5] and Ar, Kr, and Xe are partially mobile in photoresist films, their mobility being strongly dependent on the mass of the implanted ion.

The above results suggested a systematic study of the diffusional behavior of noble gases when implanted into polymers. Recently, we found that when Xe is implanted into a photoresist film[8] at slow temperature (90 K), we get a regular range profile with range parameters well reproduced by the theory. However, successive annealings performed up to 293 K revealed the existence of two diffusional processes: a slow one in the near-surface region (region damaged by the implantation process) which can be explained by a trapping-detrapping mechanism, and a regular rapid one in the deeper zone which is responsible for the appearance of a penetrating tail directed toward the bulk. The obtained diffusion coefficients follow an Arrhenius behavior characterized by a rather low activation energy $E_b = 80$ meV.

On the other side, it was recently reported that Ar irradiated Xe implanted samples have undergone a quite noticeable radiation induced diffusion process.[9] Then, it is interesting to complete this study in order to compare the thermal diffusion results with the ones obtained from ion radiation.

With this aim we have undertaken the present work, where we have performed a systematic study of the different parameters which can influence the radiation induced diffusion mechanism. We have implanted AZ1350 photoresist films with Xe ions, then we have Ar irradiated the implanted samples at different fluences. Furthermore, we have changed the Xe implantation dose and also the post-bombarding ion species. In this way we were able to gain information on the influence of important parameters, such as the irradiation and implantation doses and projectile species on the radiation induced diffusion mechanism.

All the Xe depth profiles were measured using the Rutherford backscattering technique with α particles at 760 keV.

II. EXPERIMENTAL PROCEDURE

Clean silicon wafers were spin coated with an AZ1350 photoresist film of 1.5 μm thickness and then baked for 20 min at 90 °C. Small pieces of the wafers (~ 4 cm^2) were subsequently implanted with 10^{14}, 5×10^{14}, 8×10^{14}, and 10^{15} Xe atoms/cm^2 at 80 keV. Post-irradiations were performed with Ne, Ar, Kr, and Xe ions in the 670–800 keV range with doses ranging from 5×10^{13}, up to 2×10^{15} atoms/cm^2. All the implantations and irradiations were done at room temperature at the 400 kV ion implanter of the Institute of Physics, Porto Alegre. The beam current densities were in all cases well below 50 nA/cm^2, so that sample heating by the ion beam can be excluded.

Depth profiles were obtained via RBS analysis using 760 keV particles from the same implanter. Backscattered particles were registered by a silicon surface barrier detector placed at 160° with respect to the α beam direction. The overall resolution of the system was better than 14 keV. The beam spot on the sample was changed whenever the α dose reached 2×10^{12} atoms/cm^2. This procedure was followed to avoid compactation effects and formation of carbon-rich regions as a consequence of large irradiation fluence. The energy-to-depth transformation was done using the α stopping powers, as reported in Ref. 3.

 0021-8979/92/235139-06$04.00

III. DATA EVALUATION

In order to analyze the present data, we have assumed that the radiation induced diffusion follows a trapping-detrapping mechanism. In fact, the implantation process produces a damage in the photoresist, which according to the Monte Carlo TRIM code calculation[4] goes from the surface up to about α 500 Å. In this region, the implanted ions can be trapped by the damage centers. In the framework of our model, we assume that the detrapping is produced by the ion bombardment so the diffusion process undergoes a trapping-detrapping mechanism. In the deeper zone, the trapping probability is zero because of two reasons: first, due to the absence of damage produced by the implantation process, and second, because the noble gases cannot be chemically bound to the components of the photoresist (as happens with other elements like Bi, Cs, Sn, Fe, etc.).

Therefore, we have assumed a model where there exists only one kind of trap homogeneously distributed in the damaged region as calculated by the TRIM program.

Let us define B as the probability rate for ion detrapping and A as the probability rate for ion trapping. Then, the differential equations which have to be solved are

$$\frac{\delta C_f}{\delta t}=D\frac{\delta^2 C_f}{\delta x^2}-AC_f+BC_t \quad C_f=C_f(x,t), \tag{1}$$

$$\frac{\delta C_t}{\delta t}=AC_f-BC_t \quad C_t=C_t(x,t), \tag{2}$$

where C_f and C_t denote the concentration of free and trapped atoms, respectively. In addition,

$$C=C_f+C_t,$$

where C denotes the total ion concentration.

In order to solve the differential equations (1) and (2) we have used a numerical approach, the so called "finite difference method."[10] In this approach, the whole depth profile of a given distribution is divided into single channels. The diffusion of the particles of each channel is treated individually, and the product of all diffused contributions of each channel are summed up in order to construct the new profile. This procedure is run iteratively for many individual diffusion steps until the total required mobility is reached. Further details of the method can be found, for example, in Ref. 11.

IV. EXPERIMENTAL RESULTS

In the present experiment, we have studied the influence of the different parameters on the radiation induced diffusion mechanism such as: (a) the ion implantation fluence, (b) the ion post-bombarding fluence, and (c) the influence of the ion species used in the irradiation experiments. In the following, those relations are described separately.

A. Dependence on the bombarding fluence

After the implantation of the AZ1350 sample with a Xe fluence of $\phi=8\times10^{14}$ Xe/cm^2 (at 80 keV), we have performed the irradiation experiments with 760 keV Ar ions, with fluences ranging from $\phi=5\times10^{13}$ Ar/cm^2 up to $\phi=2\times10^{15}$ Ar/cm^2. The corresponding RBS spectra are displayed in Fig. 1. It clearly can be seen that the Ar irradiation induces Xe diffusion. This feature was observed even for the lowest bombarding dose $\phi=5\times10^{13}$ Ar/cm (not shown in the figure). Moreover, it can also be observed that the increase of the bombarding fluence decreases the Xe peak, indicating that the trapped ions diffuse out of the implanted region. It should be mentioned that each irradiation experiment was performed with a freshly Xe implanted sample.

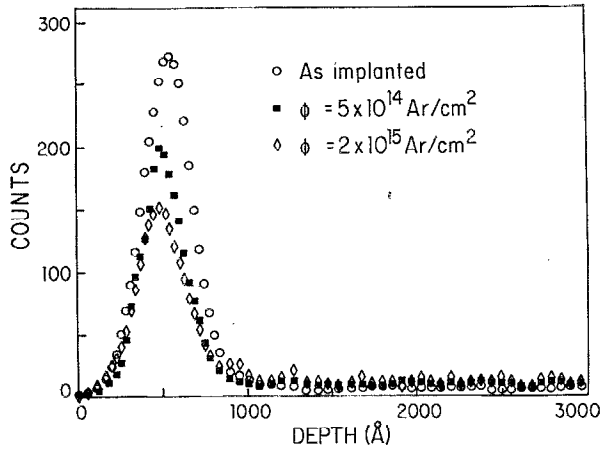

FIG. 1. RBS spectra of: (a) Xe implanted sample at 80 keV, $\phi=8\times10^{14}$ atoms/cm^2, (b) same as before but postbombarded with Ar, 760 keV, $\phi=5\times10^{14}$ atoms/cm^2 (squares), and (c) as (a) but postbombarded with Ar, 760 keV $\phi=2\times10^{15}$ atoms/cm^2.

B. Influence of the implantation dose

We have studied the influence of the damage produced by the implantation process on the radiation induced diffusion mechanism. In this connection, we have repeated the Ar bombardment experiments described above for three different Xe implanted fluences $\phi=5\times10^{14}$, 8×10^{14}, and 10^{15} Xe/cm^2 at 80 keV.

The results of the present experiments show that the fraction of Xe ions which diffuse out of the implanted region (for a given Ar irradiation dose) is strongly dependent on the Xe implanted fluence. A typical example of this behavior is shown in Fig. 2. In the figure, the depth profile of the as-implanted sample (Xe dose $\phi=5\times10^{14}$ Xe/cm^2) is displayed together with the corresponding post-bombarded one (760 keV Ar ions at $\phi=5\times10^{14}$ Ar/cm^2). In the present case almost 50% of the Xe implanted ions have diffused out of the implanted zone as a consequence of the post-irradiation process. This number is much higher than the one obtained in the experiment, whose results are shown in Fig. 1. In the later case, for a Xe implantation dose of $\phi=8\times10^{14}$ and the same Ar irradiation fluence ($\phi=5\times10^{14}$ Ar/cm^2), only 33% of the Xe implanted ions have left the implanted region.

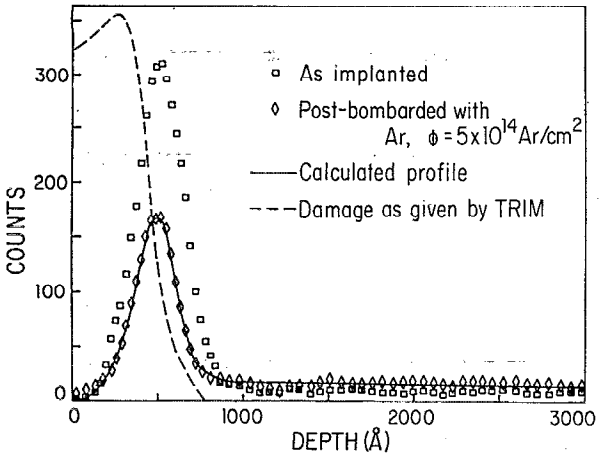

FIG. 2. RBS spectra of: (a) as-implanted Xe sample ($E=80$ keV, $\phi=5\times10^{14}$ atoms/cm^2) (squares), (b) postbombarded with Ar, $\phi=5\times10^{14}$ atoms/cm^2, triangles. The dashed line indicates the calculated TRIM damage profile. The full line indicates the calculated profile.

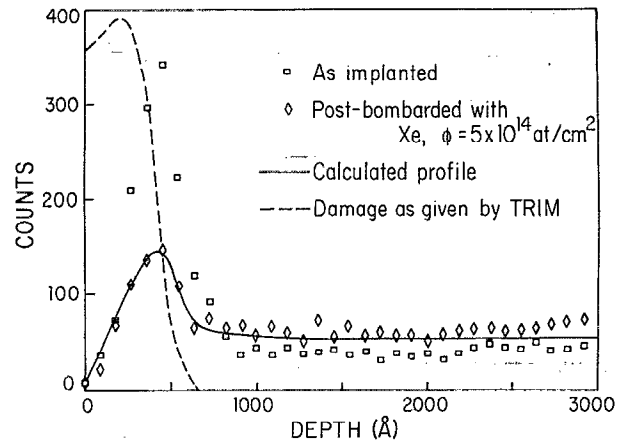

FIG. 3. RBS spectra of: (a) as-implanted Xe (80 keV, $\phi=5\times10^{14}$ atoms/cm^2) (squares), (b) postbombarded with Xe ($E=800$ keV, $\phi=5\times10^{14}$ atoms/cm^2) (triangles). The dashed line indicates the TRIM calculated damage profile. The full line indicates the calculated profile.

The influence of both the irradiation and implantation doses on the radiation induced diffusion mechanism can be more easily seen by evaluating data, as described in Sec. III. This procedure is illustrated in Fig. 2. The dashed line indicates the total (nuclear and electronic) damage profile produced by the implantation process as calculated by TRIM. Then, we have chosen the trapping profile porportional to the damage profile. It was found that the trapping probability rate $A=8\times10^{-4}$ s^{-1} and a detrapping rate $B=2.5\times10^{-5}$ s^{-1} lead to the best fit of the measured profiles. Starting from the initial profile (squares), the program provides the ion distribution shown with full line. As can be observed, the agreement between the calculated and experimental profiles (losange) is quite satisfactory. The extracted Dt parameter is $Dt=6.2\times10^{-10}$ cm^2.

This procedure has been applied for each implanted Xe fluence for all the Ar irradiation doses. The parameters used as input for the diffusion program and the obtained Dt coefficients are shown in Table I.

An inspection of Table I shows three interesting features. First the Dt parameter (which is proportional to the square of the diffusion length) is dependent on the Ar irradiation dose. Second, the detrapping probability B is independent of both the irradiation and implantation doses. Third, the trapping probability is only dependent on the Xe implantation dose.

C. Dependence on irradiation projectile species

Next, we have studied the dependence of the Xe diffusion on the irradiated ion species. With this purpose we have selected Ne, Kr, and Xe, in addition to Ar as postbombarding ions. The irradiation energies were chosen so that the electronic energy loss of the projectiles was maintained constant (within ±10%). On the other side, the

TABLE I. Compilation of results for the Ar irradiation experiments. The Xe implanted energy was fixed at 80 keV. The Dt, A, and B parameters are extracted from the calculated diffusion profiles.

Fluence (10^{14} ions/cm^2)			Diffusion parameters	
Implantation Xe	Irradiation Ar	Dt (10^{-10} cm^2)	Trapping rate (A) (10^{-3} s^{-1})	Detrapping rate (B) (10^{-5} s^{-1})
5	0.5	1	0.8	2.5
	1	4.1	0.8	2.5
	5	6.2	0.8	2.5
	20	11.6	0.8	2.5
8	0.5	1.9	1.3	2.5
	1	3.7	1.3	2.5
	5	6.2	1.3	2.5
	20	8	1.3	2.5
10	0.5	1.5	1.6	2.5
	1	2	1.6	2.5
	5	4.9	1.6	2.5
	20	9	1.6	2.5

TABLE II. Compilation of results for the irradiation experiments performed with different kind of ions. The Dt, A, and B parameters were extracted from the calculated diffusion profiles.

Ion	Energy (keV)	Nuclear stopping Sn (eV/Å)	Electronic stopping Se (eV/Å)	Dt (10^{-10} cm^2)	A (10^{-4} s^{-1})	B (10^{-5} s^{-1})
Ne	60	15	22	5.6	7.8	2.6
	760	3	75	5	8	2.1
Ar	670	15	77	6	8	2.5
Kr	760	62	63	8	8	3
Xe	800	125	70	15	8	3.8

nuclear energy transfer was changed over a wide range (3 eV/Å $<$ Sn $<$ 120 eV/Å), see Table II.

In Fig. 3 are shown the RBS spectra of the as-implanted Xe sample, and of the one postbombarded with 800 keV Xe ions ($\phi = 5\times10^{14}$ Xe/cm^{-2}). In this case, the irradiation produces a drastic effect, since more than 65% of the implanted ions have diffused out of the implanted region. In order to extract the characteristic parameters of the diffusion process, we have proceeded as before. The dashed line corresponds to the TRIM damage profile, the squares represent the original Xe profile, the losanges, the postbombarded one, and the full line corresponds to the calculated profile.

The input and the extracted diffusion parameters are compiled in Table II. Also in the same table are quoted the energies employed for each ion, and the corresponding electronic and nuclear stopping powers.

Inspection of Table II shows that the trapping probability A is independent of the ion used for the postbombarding experiment but depends on the implantation dose. On the other side, the detrapping probability B increases with increasing ion mass. This feature is more clearly depicted in Fig. 4, where we have plotted the detrapping probability rate B as a function of the transferred nuclear energy density Sn. It can be observed that B is proportional to the transferred nuclear energy density.

In addition, we have performed one experiment with Ne where the irradiation energy (60 keV) was chosen in a way that it gives the same nuclear stopping power as Ar at 670 keV (Sn = 15 eV/Å), but an electronic stopping power which is 3.5 times lower than the one for Ar. The similarity of the diffusional parameters A, B, and Dt of both experiments (see Table II) indicates that the electronic energy transfer processes seems to play a minor role for the diffusional process.

V. DISCUSSION

Our experiment shows several interesting features that we would like to discuss separately.

A. Irradiation effect

In Fig. 5 are plotted the diffusional lengths $\sqrt{Dt}$, obtained in the present experiment (for each implanted Xe dose) as a function of the Ar irradiated fluence. An inspection of the figure shows two interesting features: first, the diffusion length parameters seems to be independent of the Xe implantation dose. In fact, for $\phi = 5\times10^{13}$ Ar/cm^2 the differences in the obtained $\sqrt{Dt}$ values are less than 20%, while for the highest fluence ($\phi = 2\times10^{15}$ Ar/cm^2), this difference is reduced to less than 10%. Since the uncertainties in the extracted $\sqrt{Dt}$ parameters are of the order of $\sim$15%, it can be concluded that the above differences are within our experimental error.

A second interesting feature is that the $\sqrt{Dt}$ follows a ϕ^{α} ($\alpha = 0.22$) relationship with the Ar bombarding dose.

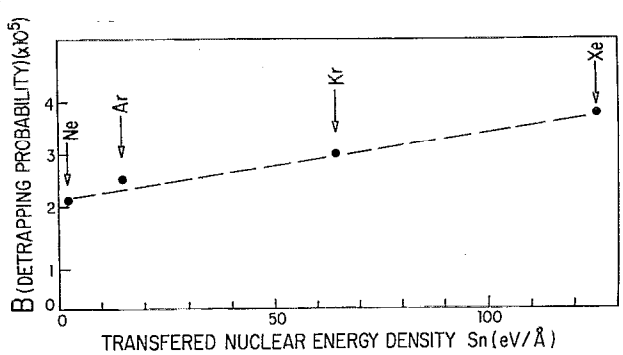

FIG. 4. Detrapping probability rate B as a function of the nuclear energy transfer. The broken line is only to guide the eye.

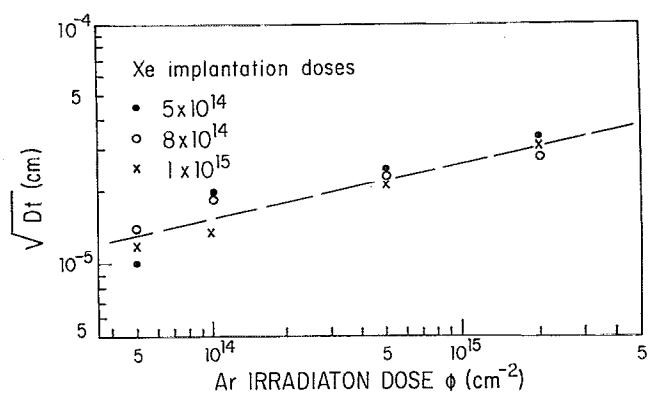

FIG. 5. Diffusion length parameters $\sqrt{Dt}$ as a function of the irradiated fluence, for each implanted fluence.

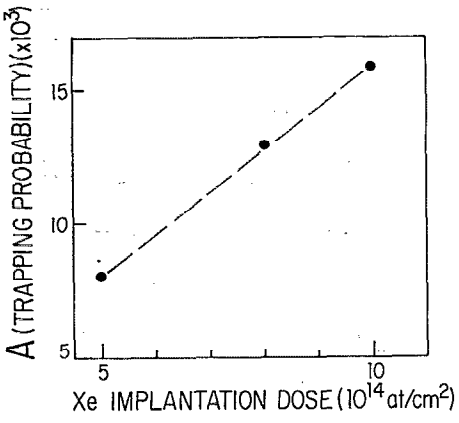

FIG. 6. Trapping probability rate A as a function of the Xe implanted dose. The line is only to guide the eye.

At the same time, for a given Xe implantation fluence, the A and B parameters remain constant. This implies that the irradiation process induces a diffusion mechanism with diffusion lengths increasing with the fluence, with the trapping and detrapping probability rates being independent of the bombarding fluence.

The present results can be converted to diffusivities D as $t=\phi/\dot{\phi}$ ($\dot{\phi}$ is the ion flux). For Xe implanted at $\phi=5\times10^{14}$ Xe/cm^2 and postbombarded with Ar, $\phi=5\times10^{14}$ Ar/cm^2, one obtains $D=1.7\times10^{-13}$ cm^2/s (see Table I). This number should be compared with the one extracted from the low-temperature thermal diffusion study of Xe implanted in the same AZ1350 polymer.[8] In this work, it was found that at 293 K the diffusional process is characterized by $D=1.3\times10^{-14}$ cm^2/s. We see that the irradiation produces a moderate enhancement of the Xe mobility. In fact, this enhanced mobility corresponds to a purely thermal diffusion at around 600 K. Due to the low ion flux applied we can exclude that the ion beam sample heating would be responsible for the observed enhanced mobility.

A second result that can be found is that the trapping probability A is directly proportional to the implantation dose. This feature is shown in Fig. 6. However, it should be stressed that this relationship is only valid within the limited studied fluence range. One expects that, for higher implantation doses, this relationship should saturate due to saturating damage.

It is known that the trapping probability A is related to the defect concentration via $A\equiv4\pi r_s D C_s(1)$ where r_s is the effective trapping radius, D is the diffusion coefficient, and C_s is the concentration of trapping centers. Taking a typical value for A, $A=8\times10^{-4}$ s^{-1} (for $\phi=5\times10^{14}$ Xe/cm^2) and assuming that $r_s\cong10^{-8}$ cm, one arrives to the conclusion that 10^{17} cm^{-3} trapping centers have been formed in the implanted area. This number should be compared with the one provided by the TRIM program which gives for the defect density $C_d=10^{22}$ defects/cm^3. The difference between the measured trap concentration C_s and the calculated defect concentration C_d indicates that not all the damage produced by the implantation produces traps for the Xe implanted ions.

On the other side, the detrapping probability can be written as $B=v_t\exp(-E_t/KT)$ where v_t is the jump frequency of the atoms and E_t is the activation energy for the detrapping process. Assuming that $v_t=10^{13}$ ℓ/s, one obtains that at room temperature, $E_t\cong1.0$ eV. This number is much larger (~10 times) than the thermal activation energy Eb (80 meV), obtained in the low temperature diffusion experiment. This estimation is based on the value v_t which is typical for metals. Any higher frequency is going to give higher detrapping binding energy.

B. Mass effect

It was shown—Fig. 4—that the detrapping probability rate is linearly related to the nuclear transfer energy mechanism. This dependence is not strong, since an increase by a factor of 40 in the ϵ_n value produces only a variation of two in the detrapping probability rate B. On the other side it was shown that the electronic transfer energy plays a minor role in the detrapping mechanism–see Table II.

This means that we encounter here one of the few processes where the nuclear energy transfer mechanism is dominant for polymers instead of the electronic one. Other physical polymer properties which seem to be essentially affected by nuclear processes are, e.g., the optical blackening of polymers[12] and their surface degradation,[13] when implanted at relatively low projectile energies.

This has to be compared with, e.g., the electronic polymer conductivity,[14] the chemical etchability of polymers,[15] the depth profiles of depletion of their volatile components after ion irradiation,[1] the optical refractive index changes,[16] or the redistribution profiles of light implanted elements,[2,17] which all scale with the electronic energy transfer distributions.

VI. CONCLUSIONS

We have assumed a model where the radiation induced diffusion follows a trapping-detrapping mechanism. In the framework of this model, which reproduces quite well the experimental results, we have found several interesting features. First, the diffusion length $\sqrt{Dt}$ depends on the irradiation dose, following a power law independent of the damage produced by the implantation process. The ion irradiation produces a moderate enhancement of the Xe mobility equivalent to a purely thermal process of around 600 K.

In the second place, it could be observed that the trapping probability A is directly proportional to the damage produced by the implantation process. However, it seems that not all the produced damage centers act as trapping centers. Their efficiency is of the order of 10^{-5}. On the other side, it was also found that the detrapping process needs (at least) an energy of 1.0 eV, which is three times higher than the pure thermal one.

Finally, it seems that the nuclear energy transfer is the main mechanism in producing the detrapping and so the radiation induced process. As was mentioned above, this is one of the few processes where the nuclear transfer mechanism is dominant for polymers.

It will be an important task in the future to understand why for one mechanism the nuclear and in the other case the electronic energy transfer plays the essential role.

[1] R. B. Guimarães, M. Behar, R. P. Livi, J. P. de Souza, F. C. Zawislak, D. Fink, and J. P. Biersack, J. Appl. Phys. **60**, 1322 (1986).

[2] R. B. Guimarães, M. Behar, R. P. Livi, J. P. de Souza, L. Amaral, F. C. Zawislak, D. Fink, and J. P. Biersack, Nucl. Instrum. Methods **19/20**, 882 (1987).

[3] J. F. Ziegler, J. P. Biersack, and U. Littmark, in *Stopping and Range of Ions in Solids*, edited by J. F. Ziegler (Pergamon, New York, 1985), Vol. 1.

[4] J. P. Biersack and L. G. Haggemark, Nucl. Instrum. Methods **174**, 257 (1980).

[5] D. Fink, M. Müller, U. Sttetner, M. Behar, P. F. P. Fitchner, F. C. Zawislak, and S. Koul, Nucl. Instrum. Methods B **32**, 150 (1988).

[6] R. B. Guimarães, L. Amaral, M. Behar, P. F. P. Fichtner, F. C. Zawislak, and D. Fink, J. Appl. Phys. **63**, 2083 (1988).

[7] R. B. Guimarães, L. Amaral, M. Behar, F. C. Zawislak, and D. Fink, Nucl. Instrum. Methods B **39**, 800 (1989).

[8] M. Behar, L. Amaral, J. R. Kaschny, and F. C. Zawislak, Phys. Lett. A **148**, 104 (1990).

[9] M. Behar, L. Amaral, J. R. Kaschny, F. C. Zawislak, and D. Fink, Nucl. Instrum. Methods B **39**, 800 (1989).

[10] G. D. Smith, *Numerical Solution of Partial Differential Equations: Finite Difference Methods*, 2nd ed. (Clarendon, Oxford, 1978).

[11] M. Behar, R. B Guimarães, P. L. Grande, L. Amaral, J. P. Biersack, D. Fink, J. R. Kaschny, and F. C. Zawislak, Phys. Rev. B **41**, 6145 (1990).

[12] D. Fink, M. Müller, L. T. Chadderton, P. H. Cannington, R. G. Elliman, and D. C. McDonald, Nucl. Instrum. Methods B **32**, 125 (1988).

[13] S. Koul, I. D. Campbell, D. C. McDonald, L. T. Chadderton, D. Fink, J. P. Biersack, and M. Müller, Nucl. Instrum. Methods B **32**, 186 (1988).

[14] J. Davenas, X. L. Xu, G. Boiteux, and D. Sage, Nucl. Instrum. Methods B **39**, 754 (1989).

[15] S. L. Koul, I. D. Campbell, L. T. Chadderton, M. Langroo, D. Fink, and J. P. Biersack, Nucl. Instrum. Methods B **32**, 383 (1988).

[16] J. P. Biersack and R. Kallweit, Nucl. Instrum. Methods B **46**, 309 (1990).

[17] R. B. Guimarães, L. Amaral, M. Behar, F. C. Zawislak, and D. Fink, Nucl. Instrum. Methods B **39**, 800 (1989).